

High-order fluctuations of temperature in hot QCD matter

Jinhui Chen,^{1,2,*} Wei-jie Fu,^{3,†} Shi Yin,^{4,‡} and Chunjian Zhang^{1,2,§}

¹Key Laboratory of Nuclear Physics and Ion-beam Application (MOE), and
Institute of Modern Physics, Fudan University, Shanghai 200433, P.R. China

²Shanghai Research Center for Theoretical Nuclear Physics, NSFC and Fudan University, Shanghai 200438, P.R. China

³School of Physics, Dalian University of Technology, Dalian, 116024, P.R. China

⁴Institut für Theoretische Physik, Justus-Liebig-Universität Gießen, 35392 Gießen, Germany

A new thermodynamic state function is introduced to describe the thermodynamics relevant for the mean transverse momentum fluctuations of charged particles in heavy-ion collisions, which allows us to compute the temperature fluctuations of different orders in hot quantum chromodynamics (QCD) matter for the first time. Consequently, it is found that the temperature fluctuations are suppressed remarkably as the system transitions from the hadron resonance gas (HRG) to the quark-gluon plasma (QGP) with increasing temperature or baryon chemical potential, alongside a negative skewness. This is attributed to the general fact that the heat capacity of QCD matter increases significantly in QGP in comparison to that in HRG. These predictions provide a unique signature to discover the thermodynamical temperature fluctuations in upcoming heavy-ion collision experiments, which also paves a novel way to study QCD thermodynamics and QCD phase diagram through measurements of the mean transverse momentum fluctuations of charged particles.

Introduction. An exotic state of matter, the quark-gluon plasma (QGP), characterized by color deconfinement and restoration of chiral symmetry, was believed to form in relativistic heavy-ion collisions [1, 2]. Looking for the signatures of QGP and studying its properties have been one of the main physics of the high energy nuclear physics facilities [3–7]. The occurrence of a phase transition from the QGP to a hadron resonance gas (HRG) or the existence of a critical end point in the phase diagram of QCD matter [8–12] may potentially be revealed by measurements of thermodynamic fluctuations [13–15], such as net-baryon or net-proton number fluctuations [16–24] and temperature fluctuations [25]. Event-by-event (EbE) fluctuations in charged particle momentum distributions serve as probes of thermalization and the statistical nature of particle production in such collisions [26–30].

Recent advances in heavy-ion collision experiments now enable the isolation of the thermal fluctuations from confounding effects, such as the initial state geometry fluctuations [31–35], flow contributions, and other non-thermal sources, allowing the direct measurements of thermodynamical properties of hot QCD matter [36], e.g., the speed of sound [37–39]. High-order thermodynamical quantities, e.g., the temperature fluctuations, could also be used to probe the QCD thermodynamics and phase transitions, since they are more sensitive to the critical fluctuations, i.e. the singular part of the thermodynamic potential during the phase transition in comparison to low-order thermodynamical quantities, such as the temperature itself [40–43]. This is similar with the case of ordinary net-proton number fluctuations. In

principle, temperature fluctuations can be extracted from EbE mean transverse momentum fluctuations of final-state charged particles [25], isolated from other effects, e.g., the hydrodynamic effect [44]. To that end, one has to study the thermodynamical properties of temperature fluctuations from the theoretical side, in particular the smoking-gun signature of temperature fluctuations, in measurements of EbE mean transverse momentum fluctuations that have been extensively done across collision energies and systems in various heavy-ion facilities [34, 45–50].

We develop a theoretical framework to systematically investigate temperature fluctuations in hot QCD matter, which is general and applicable to temperature fluctuations of arbitrary order. As a specific application, this approach is applied to the QCD thermodynamics described by a 2+1 flavor low energy effective field theory (LEFT) [51], where quantum and thermal fluctuations are encoded self-consistently through the functional renormalization group (fRG). The fRG has proven to be a powerful nonperturbative theoretical method, and is well suited for the studies of properties of the hot QCD matter including the QCD phase diagram, critical end point, and real-time dynamics, etc., see Refs. [10, 52–57].

We first introduce a new thermodynamic state function to characterize the thermodynamics related to the mean transverse momentum fluctuations of charged particles, from which we derive analytic expressions for the temperature fluctuations to arbitrary order. Numerical results are obtained by applying this framework to a 2+1 flavor LEFT within the fRG approach. Our approach demonstrates that temperature fluctuations would be suppressed remarkably as the matter evolved from HRG to QGP with the increase in temperature or the baryon chemical potential.

A new thermodynamic state function. We begin with

* chenjinhui@fudan.edu.cn

† wjfu@dlut.edu.cn

‡ Shi.Yin@theo.physik.uni-giessen.de

§ chunjianzhang@fudan.edu.cn

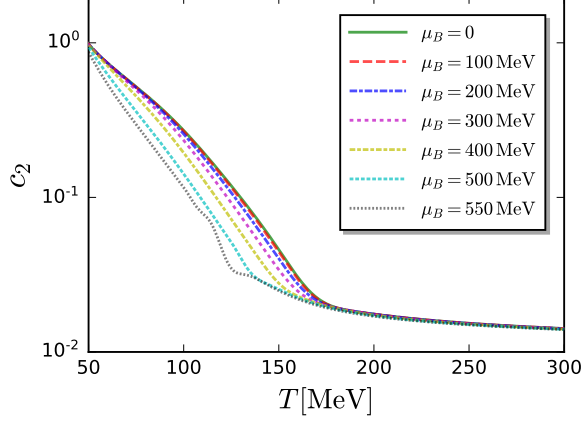


FIG. 1. Variance of temperature fluctuations as a function of the temperature with several different values of baryon chemical potential.

a total derivative of the thermodynamic potential Ω

$$d\Omega = -SdT - pdV - N_B d\mu_B, \quad (1)$$

with the entropy S , temperature T , pressure p , volume V , baryon number N_B , and the baryon chemical potential μ_B . Although we explicitly show μ_B as a representative of the conserved charge, Eq. (1) is readily generalized to include additional chemical potentials when other conserved charges are presented. The thermodynamic potential Ω is a state function of T , V and μ_B . By implementing a Legendre transformation upon Ω w.r.t. the conjugate pair S and T , we introduce a new state function as

$$W = \Omega + TS. \quad (2)$$

One immediately recognizes that there is another relation for the state function W , that is,

$$W = U - \mu_B N_B, \quad (3)$$

resulting from the general thermodynamical relations, where U denotes the energy. Inserting Eq. (2) into Eq. (1), one arrives at

$$dW = TdS - pdV - N_B d\mu_B, \quad (4)$$

indicating that W is a state function of S , V and μ_B .

In experimental measurements of mean transverse momentum fluctuations, finite acceptance cuts in the rapidity (y) and transverse momentum (p_T) range are applied, which signifies that the system volume and the chemical potential in Eq. (4) are approximately constant. While this approximation holds for high-energy collisions, we note that μ_B may vary in low-energy regions, e.g., fixed target collisions at RHIC, due to global baryon number conservation effects [23, 58, 59]. For the present study,

we neglect these corrections and maintain the constant approximation.

Recent measurements of mean transverse momentum fluctuations at RHIC and the LHC are performed at a fixed multiplicity of charged particles N_{ch} , as shown in Ref. [34, 50, 60, 61]. Since N_{ch} scales directly with the entropy of the system ($N_{\text{ch}} \sim S$). Consequently, the state function W in Eq. (4) becomes the appropriate thermodynamic potential to describe these experimental observables, since its natural variables correspond directly to the constrained quantities in the measures.

Temperature fluctuations derivations. Having established the relevance of the state function W in Eq. (4) for heavy-ion collisions, we now derive the temperature fluctuations, or equivalently, the mean transverse momentum fluctuations of charged particles, computed from the derivative of W w.r.t. S for different orders.

For a fixed volume V , we define the intensive quantities: the thermodynamic potential density $w = W/V$ and the entropy density $s = S/V$, one arrives at

$$w = -p + Ts, \quad (5)$$

where $\Omega = -pV$ is used and the entropy density can be obtained from $s = \frac{\partial p}{\partial T}$. The first-order derivative of w w.r.t. s produces the temperature

$$\frac{\partial w}{\partial s} = T. \quad (6)$$

Then, the n -th order fluctuation of temperature is obtained from the n -th order derivatives of w w.r.t. s , to wit,

$$\langle (\Delta T)^n \rangle = T^{4n-4} \frac{\partial^n w}{\partial s^n}, \quad (7)$$

with $\Delta T = T - \langle T \rangle$ and $n \geq 2$ ($n \in \mathbb{Z}$), where $\langle \dots \rangle$ denotes the ensemble average. It is convenient to adopt a dimensionless temperature fluctuation

$$c_n = \frac{\langle (\Delta T)^n \rangle}{T^n}. \quad (8)$$

The cumulants c_n can be expressed in terms of temperature derivatives of the pressure through fundamental thermodynamic relations. The first three nontrivial orders corresponding to the variance, skewness, and kurtosis of temperature fluctuations, are given by,

$$\begin{aligned} c_2 &= T^2 \left(\frac{\partial^2 p}{\partial T^2} \right)^{-1} \\ c_3 &= -T^5 \left(\frac{\partial^2 p}{\partial T^2} \right)^{-3} \frac{\partial^3 p}{\partial T^3} \\ c_4 &= T^8 \left[3 \left(\frac{\partial^2 p}{\partial T^2} \right)^{-5} \left(\frac{\partial^3 p}{\partial T^3} \right)^2 - \left(\frac{\partial^2 p}{\partial T^2} \right)^{-4} \frac{\partial^4 p}{\partial T^4} \right]. \end{aligned} \quad (9)$$

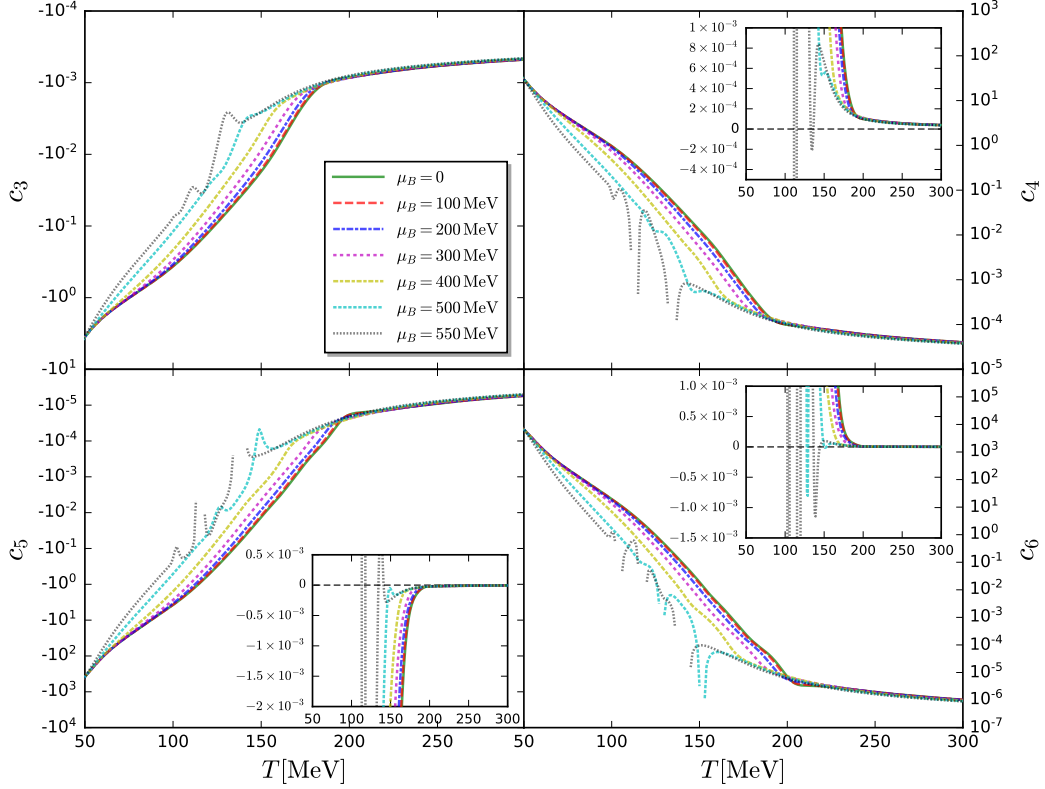


FIG. 2. High-order temperature fluctuations of the third through sixth orders, i.e., c_n in Eq. (8), as functions of the temperature with several different values of baryon chemical potential. The insets show the respective plot by using the linear y -axis, where the zero-crossing is clear.

This systematic approach can be extended to higher-order cumulants, e.g., the fifth and sixth hyper-order ones, which read

$$\begin{aligned}
 c_5 = & T^{11} \left[-15 \left(\frac{\partial^2 p}{\partial T^2} \right)^{-7} \left(\frac{\partial^3 p}{\partial T^3} \right)^3 - \left(\frac{\partial^2 p}{\partial T^2} \right)^{-5} \frac{\partial^5 p}{\partial T^5} \right. \\
 & \left. + 10 \left(\frac{\partial^2 p}{\partial T^2} \right)^{-6} \frac{\partial^3 p}{\partial T^3} \frac{\partial^4 p}{\partial T^4} \right] \\
 c_6 = & T^{14} \left[105 \left(\frac{\partial^2 p}{\partial T^2} \right)^{-9} \left(\frac{\partial^3 p}{\partial T^3} \right)^4 - 105 \left(\frac{\partial^2 p}{\partial T^2} \right)^{-8} \right. \\
 & \times \left(\frac{\partial^3 p}{\partial T^3} \right)^2 \frac{\partial^4 p}{\partial T^4} + 10 \left(\frac{\partial^2 p}{\partial T^2} \right)^{-7} \left(\frac{\partial^4 p}{\partial T^4} \right)^2 \\
 & \left. + 15 \left(\frac{\partial^2 p}{\partial T^2} \right)^{-7} \frac{\partial^3 p}{\partial T^3} \frac{\partial^5 p}{\partial T^5} - \left(\frac{\partial^2 p}{\partial T^2} \right)^{-6} \frac{\partial^6 p}{\partial T^6} \right]. \quad (10)
 \end{aligned}$$

Numerical results. We investigate QCD thermodynamics employing a 2+1 flavor LEFT within the fRG approach. As demonstrated in Ref. [51], this approach

yields an equation of state (EoS) and baryon number fluctuations consistent with lattice QCD calculations. The setup of our LEFT is also recapitulated in the supplemental materials of this Letter.

To proceed, we systematically calculate the temperature derivatives of pressure:

$$\chi_n = T^{n-4} \frac{\partial^n p}{\partial T^n}, \quad (11)$$

which is dimensionless by means of normalization with appropriate powers of T . From the state function Ω in Eq. (1), we identify the first and second order derivatives, χ_1 and χ_2 , are just related to the entropy and heat capacity, respectively. Higher-order χ_n ($n \geq 2$) can be interpreted as entropy fluctuations of different orders. The numerical results of χ_n from the first to sixth orders calculated in the 2+1 flavor LEFT-fRG framework are presented in the supplement. We found that the entropy fluctuations increase and oscillate near the chiral crossover, and the strength and amplitude of the oscillation increase with the order of fluctuations or the value of the baryon chemical potential.

The temperature fluctuations in Eq. (8) can be reformulated in terms of χ_n , defined in Eq. (11). For the

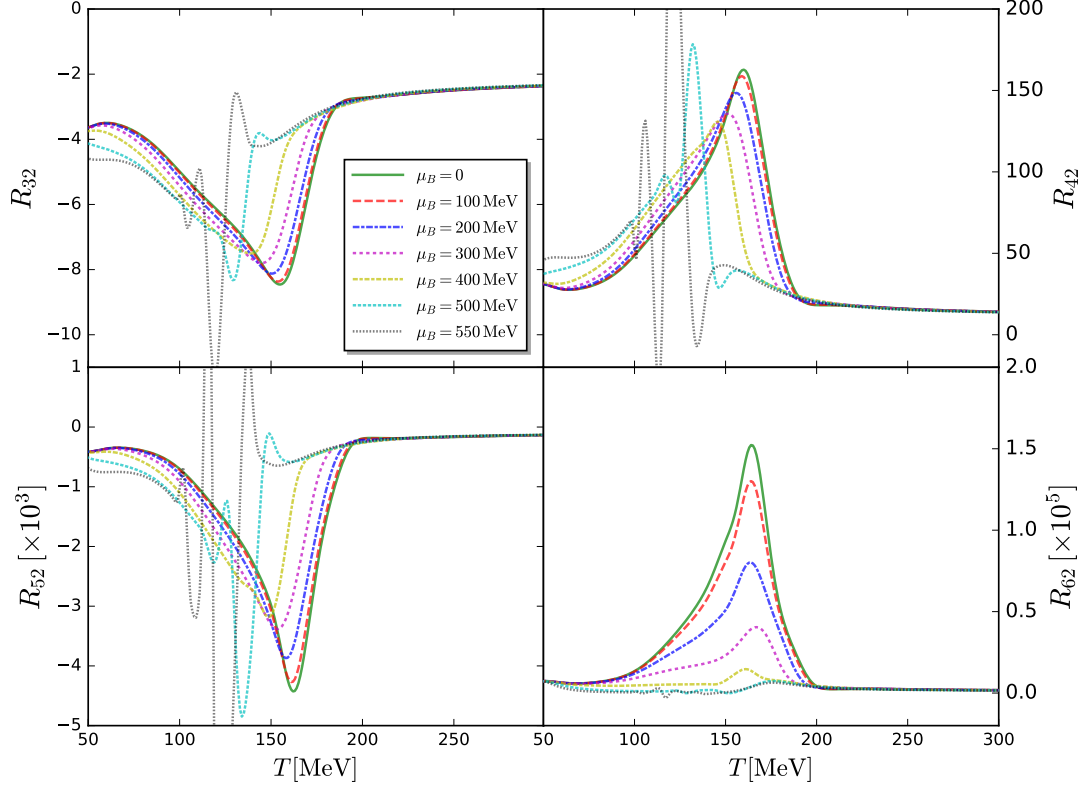


FIG. 3. Ratios between high-order temperature fluctuations and the variance, $R_{32} = c_3/c_2^2$, $R_{42} = c_4/c_2^3$, $R_{52} = c_5/c_2^4$, $R_{62} = c_6/c_2^5$, as functions of the temperature with several different values of baryon chemical potential.

lowest-order cumulants, we obtain

$$c_2 = \frac{1}{\chi_2}, \quad c_3 = -\frac{\chi_3}{\chi_2^3}, \quad c_4 = 3\frac{\chi_3^2}{\chi_2^5} - \frac{\chi_4}{\chi_2^4}. \quad (12)$$

The variance of temperature fluctuations, c_2 , is inversely proportional to the variance of entropy fluctuations, i.e., the heat capacity χ_2 , as demonstrated in Fig. 1. We observe that c_2 decreases with increasing temperature, reflecting the opposite trend of χ_2 as shown in the supplement. This behavior indicates a significant suppression of temperature fluctuations in QGP phase compared to those in HRG phase. The suppression is more remarkable for high-order temperature fluctuations, as is evident in Fig. 2 (note the logarithmic y -axis). A direct consequence of the suppression of temperature fluctuations at high temperature is that the distribution of temperature is wider in the region of lower temperature, which implies a negative skewness, as confirmed in the top-left panel of Fig. 2. While the kurtosis remains positive in most cases, its sign may reverse near the chiral crossover as it is sharpened continuously with the increase of baryon chemical potential. The sign change is more prominent for the hyper-order c_5 and c_6 cumulants.

In relativistic heavy-ion collisions, the event-averaged mean transverse momentum $\langle p_T \rangle$ of charged particles exhibits an approximate linear dependence on the system

temperature, $\langle p_T \rangle = aT$ [36–38, 44]. The parameter a represents the proportionality coefficient. In order to eliminate the influence from this coefficient that is not determined quite well, we instead analyze dimensionless ratios of temperature fluctuation cumulants:

$$R_{32} = \frac{c_3}{c_2^2}, \quad R_{42} = \frac{c_4}{c_2^3}, \quad R_{52} = \frac{c_5}{c_2^4}, \quad R_{62} = \frac{c_6}{c_2^5}. \quad (13)$$

where the powers of the variance in the denominators are chosen to balance the powers of T as shown in Eqs. (9) and (10). The relevant ratios, presented in Fig. 3, reveal that the cumulant ratios develop an increasingly rich nonmonotonic structure while exhibiting systematically reduced amplitudes with the increase of μ_B , reflecting competing effects where enhanced critical fluctuations near the sharpened phase boundary emerge concurrently with the overall suppression of the magnitude of temperature fluctuation, as evidenced by the behavior shown in Figs. 1 and 2.

Conclusions. We have studied temperature fluctuations in hot QCD matter through a newly introduced thermodynamic state function that directly connects to the mean transverse momentum fluctuations measured in heavy-ion collisions. Our approach yields analytic expressions for arbitrary-order temperature fluctuations, revealing their fundamental relationship with the en-

tropy, heat capacity, and high-order entropy fluctuations. Implementing this general formalism in a 2+1 flavor LEFT within the fRG, we obtain numerical results that quantify the temperature fluctuations across different thermodynamic regimes for the first time.

As the system transitions from the HRG to QGP phase with the increasing temperature or baryon chemical potential, the heat capacity of QCD matter increases substantially. This implies that a tiny change of the temperature would cost a huge amount of energy in the regime of high temperature. Therefore, the temperature tends not to change in comparison to the case in the regime of low temperature. In another word, the temperature fluctuations would be suppressed remarkably as the matter evolves from the HRG phase to the QGP phase with the increase of temperature or baryon chemical potential, as demonstrated in our calculations. The fact that temperature fluctuations at high temperature are smaller than those at low temperature leads to another direct consequence, that is, a negative skewness of temperature fluctuations. Such a signature emerges because the increasingly narrow fluctuation distribution at high temperature creates an asymmetric probability density weighted toward lower temperatures.

Note that these findings are general and model-independent. They arise from the fact that the heat capacity of the QCD matter increases significantly from

the HRG phase to the QGP phase. In the meantime, they provide a unique signature to discover the thermodynamical temperature fluctuations in upcoming heavy-ion collision experiments at e.g., RHIC-BES, FAIR-CBM, NICA, and HIAF, which also paves a novel way to study QCD thermodynamics and QCD phase diagram through measurements of the mean transverse momentum fluctuations of charged particles.

Acknowledgements. We thank Fei Gao, Xuguang Huang, Jan M. Pawłowski for discussions and comments. W.J. Fu and S. Yin also would like to thank the members of the fQCD collaboration [62] for collaborations on related projects. J.H. Chen is supported by the National Key Research and Development Program of China under Contract No. 2022YFA1604900, by the National Natural Science Foundation of China under Contract No. 12025501. W.J. Fu is supported by the National Natural Science Foundation of China under Contract Nos. 12447102, 12175030. S. Yin is supported by the Alexander v. Humboldt Foundation. S. Yin acknowledges support by the Deutsche Forschungsgemeinschaft (DFG, German Research Foundation) through the CRC-TR 211 “Strong-interaction matter under extreme conditions” – project number 315477589 – TRR 211. C. Zhang is supported by the National Natural Science Foundation of China under Contract No. 12147101, by the Shanghai Pujiang Talents Program under Contract No. 24PJJA009.

-
- [1] E. V. Shuryak, Quantum Chromodynamics and the Theory of Superdense Matter, *Phys. Rept.* **61**, 71 (1980).
 - [2] J. W. Harris and B. Muller, The Search for the quark - gluon plasma, *Ann. Rev. Nucl. Part. Sci.* **46**, 71 (1996), [arXiv:hep-ph/9602235](#).
 - [3] J. Adams *et al.* (STAR), Experimental and theoretical challenges in the search for the quark gluon plasma: The STAR Collaboration’s critical assessment of the evidence from RHIC collisions, *Nucl. Phys. A* **757**, 102 (2005), [arXiv:nucl-ex/0501009](#).
 - [4] K. Adcox *et al.* (PHENIX), Formation of dense partonic matter in relativistic nucleus-nucleus collisions at RHIC: Experimental evaluation by the PHENIX collaboration, *Nucl. Phys. A* **757**, 184 (2005), [arXiv:nucl-ex/0410003](#).
 - [5] C. W. Fabjan *et al.* (ALICE), ALICE: Physics Performance Report, *J. Phys. G* **32**, 1295 (2006).
 - [6] W. Busza, K. Rajagopal, and W. van der Schee, Heavy Ion Collisions: The Big Picture, and the Big Questions, *Ann. Rev. Nucl. Part. Sci.* **68**, 339 (2018), [arXiv:1802.04801 \[hep-ph\]](#).
 - [7] M. I. Abdulhamid *et al.* (STAR), Observation of the electromagnetic field effect via charge-dependent directed flow in heavy-ion collisions at the Relativistic Heavy Ion Collider, *Phys. Rev. X* **14**, 011028 (2024), [arXiv:2304.03430 \[nucl-ex\]](#).
 - [8] M. A. Stephanov, K. Rajagopal, and E. V. Shuryak, Signatures of the tricritical point in QCD, *Phys. Rev. Lett.* **81**, 4816 (1998), [arXiv:hep-ph/9806219](#).
 - [9] M. A. Stephanov, K. Rajagopal, and E. V. Shuryak, Event-by-event fluctuations in heavy ion collisions and the QCD critical point, *Phys. Rev. D* **60**, 114028 (1999), [arXiv:hep-ph/9903292](#).
 - [10] W.-j. Fu, J. M. Pawłowski, and F. Rennecke, QCD phase structure at finite temperature and density, *Phys. Rev. D* **101**, 054032 (2020), [arXiv:1909.02991 \[hep-ph\]](#).
 - [11] F. Gao and J. M. Pawłowski, Chiral phase structure and critical end point in QCD, *Phys. Lett. B* **820**, 136584 (2021), [arXiv:2010.13705 \[hep-ph\]](#).
 - [12] P. J. Gunkel and C. S. Fischer, Locating the critical endpoint of QCD: Mesonic backcoupling effects, *Phys. Rev. D* **104**, 054022 (2021), [arXiv:2106.08356 \[hep-ph\]](#).
 - [13] M. M. Aggarwal *et al.* (STAR), An Experimental Exploration of the QCD Phase Diagram: The Search for the Critical Point and the Onset of De-confinement, (2010), [arXiv:1007.2613 \[nucl-ex\]](#).
 - [14] A. Bzdak, S. Esumi, V. Koch, J. Liao, M. Stephanov, and N. Xu, Mapping the Phases of Quantum Chromodynamics with Beam Energy Scan, *Phys. Rept.* **853**, 1 (2020), [arXiv:1906.00936 \[nucl-th\]](#).
 - [15] J. Chen *et al.*, Properties of the QCD matter: review of selected results from the relativistic heavy ion collider beam energy scan (RHIC BES) program, *Nucl. Sci. Tech.* **35**, 214 (2024), [arXiv:2407.02935 \[nucl-ex\]](#).
 - [16] J. Adam *et al.* (STAR), Nonmonotonic Energy Dependence of Net-Proton Number Fluctuations, *Phys. Rev. Lett.* **126**, 092301 (2021), [arXiv:2001.02852 \[nucl-ex\]](#).
 - [17] M. S. Abdallah *et al.* (STAR), Measurements of Proton High Order Cumulants in $\sqrt{s_{NN}} = 3$ GeV Au+Au Collisions and Implications for the QCD Critical Point, *Phys. Rev. Lett.* **128**, 202303 (2022), [arXiv:2112.00240 \[nucl-](#)

- ex].
- [18] B. Aboona *et al.* (STAR), Beam Energy Dependence of Fifth and Sixth-Order Net-proton Number Fluctuations in Au+Au Collisions at RHIC, *Phys. Rev. Lett.* **130**, 082301 (2023), [arXiv:2207.09837 \[nucl-ex\]](#).
 - [19] M. Abdallah *et al.* (STAR), Higher-order cumulants and correlation functions of proton multiplicity distributions in sNN=3 GeV Au+Au collisions at the RHIC STAR experiment, *Phys. Rev. C* **107**, 024908 (2023), [arXiv:2209.11940 \[nucl-ex\]](#).
 - [20] Precision Measurement of (Net-)proton Number Fluctuations in Au+Au Collisions at RHIC, (2025), [arXiv:2504.00817 \[nucl-ex\]](#).
 - [21] W.-j. Fu, J. M. Pawłowski, F. Rennecke, and B.-J. Schaefer, Baryon number fluctuations at finite temperature and density, *Phys. Rev. D* **94**, 116020 (2016), [arXiv:1608.04302 \[hep-ph\]](#).
 - [22] W.-j. Fu, X. Luo, J. M. Pawłowski, F. Rennecke, R. Wen, and S. Yin, Hyper-order baryon number fluctuations at finite temperature and density, *Phys. Rev. D* **104**, 094047 (2021), [arXiv:2101.06035 \[hep-ph\]](#).
 - [23] W.-j. Fu, X. Luo, J. M. Pawłowski, F. Rennecke, and S. Yin, Ripples of the QCD critical point, *Phys. Rev. D* **111**, L031502 (2025), [arXiv:2308.15508 \[hep-ph\]](#).
 - [24] Y. Lu, F. Gao, Y.-x. Liu, and J. M. Pawłowski, Finite density signatures of confining and chiral dynamics in QCD thermodynamics and fluctuations of conserved charges, (2025), [arXiv:2504.05099 \[hep-ph\]](#).
 - [25] S. Gavin, Traces of thermalization from transverse momentum fluctuations in nuclear collisions, *Phys. Rev. Lett.* **92**, 162301 (2004), [arXiv:nucl-th/0308067](#).
 - [26] H. Heiselberg, Event-by-event physics in relativistic heavy ion collisions, *Phys. Rept.* **351**, 161 (2001), [arXiv:nucl-th/0003046](#).
 - [27] S. Jeon and V. Koch, Charged particle ratio fluctuation as a signal for QGP, *Phys. Rev. Lett.* **85**, 2076 (2000), [arXiv:hep-ph/0003168](#).
 - [28] S. A. Voloshin, V. Koch, and H. G. Ritter, Event-by-event fluctuations in collective quantities, *Phys. Rev. C* **60**, 024901 (1999), [arXiv:nucl-th/9903060](#).
 - [29] M. Asakawa, U. W. Heinz, and B. Muller, Fluctuation probes of quark deconfinement, *Phys. Rev. Lett.* **85**, 2072 (2000), [arXiv:hep-ph/0003169](#).
 - [30] L. Stodolsky, Temperature fluctuations in multiparticle production, *Phys. Rev. Lett.* **75**, 1044 (1995).
 - [31] F. G. Gardim, F. Grassi, M. Luzum, and J.-Y. Ollitrault, Mapping the hydrodynamic response to the initial geometry in heavy-ion collisions, *Phys. Rev. C* **85**, 024908 (2012), [arXiv:1111.6538 \[nucl-th\]](#).
 - [32] B. Schenke, P. Tribedy, and R. Venugopalan, Initial-state geometry and fluctuations in Au + Au, Cu + Au, and U + U collisions at energies available at the BNL Relativistic Heavy Ion Collider, *Phys. Rev. C* **89**, 064908 (2014), [arXiv:1403.2232 \[nucl-th\]](#).
 - [33] M. I. Abdulhamid *et al.* (STAR), Imaging shapes of atomic nuclei in high-energy nuclear collisions, *Nature* **635**, 67 (2024), [arXiv:2401.06625 \[nucl-ex\]](#).
 - [34] G. Aad *et al.* (ATLAS), Disentangling Sources of Momentum Fluctuations in Xe+Xe and Pb+Pb Collisions with the ATLAS Detector, *Phys. Rev. Lett.* **133**, 252301 (2024), [arXiv:2407.06413 \[nucl-ex\]](#).
 - [35] L. Zhang, J. Chen, and C. Zhang, Energy dependence of transverse momentum fluctuations in Au+Au collisions from a multiphase transport model, *Phys. Rev. C* **111**, 024911 (2025), [arXiv:2501.08209 \[nucl-th\]](#).
 - [36] F. G. Gardim, G. Giacalone, M. Luzum, and J.-Y. Ollitrault, Thermodynamics of hot strong-interaction matter from ultrarelativistic nuclear collisions, *Nature Phys.* **16**, 615 (2020), [arXiv:1908.09728 \[nucl-th\]](#).
 - [37] F. G. Gardim, G. Giacalone, and J.-Y. Ollitrault, The mean transverse momentum of ultracentral heavy-ion collisions: A new probe of hydrodynamics, *Phys. Lett. B* **809**, 135749 (2020), [arXiv:1909.11609 \[nucl-th\]](#).
 - [38] F. G. Gardim, A. V. Giannini, and J.-Y. Ollitrault, Accessing the speed of sound in relativistic ultracentral nucleus-nucleus collisions using the mean transverse momentum, *Phys. Lett. B* **856**, 138937 (2024), [arXiv:2403.06052 \[nucl-th\]](#).
 - [39] A. Hayrapetyan *et al.* (CMS), Extracting the speed of sound in quark-gluon plasma with ultrarelativistic lead-lead collisions at the LHC, *Rept. Prog. Phys.* **87**, 077801 (2024), [arXiv:2401.06896 \[nucl-ex\]](#).
 - [40] R. Arnaldi *et al.* (NA60), Evidence for the production of thermal-like muon pairs with masses above 1-GeV/c**2 in 158-A-GeV Indium-Indium Collisions, *Eur. Phys. J. C* **59**, 607 (2009), [arXiv:0810.3204 \[nucl-ex\]](#).
 - [41] J. Adamczewski-Musch *et al.* (HADES), Probing dense baryon-rich matter with virtual photons, *Nature Phys.* **15**, 1040 (2019).
 - [42] J. Churchill, L. Du, C. Gale, G. Jackson, and S. Jeon, Virtual Photons Shed Light on the Early Temperature of Dense QCD Matter, *Phys. Rev. Lett.* **132**, 172301 (2024), [arXiv:2311.06951 \[nucl-th\]](#).
 - [43] Temperature Measurement of Quark-Gluon Plasma at Different Stages, (2024), [arXiv:2402.01998 \[nucl-ex\]](#).
 - [44] G. Giacalone, F. G. Gardim, J. Noronha-Hostler, and J.-Y. Ollitrault, Skewness of mean transverse momentum fluctuations in heavy-ion collisions, *Phys. Rev. C* **103**, 024910 (2021), [arXiv:2004.09799 \[nucl-th\]](#).
 - [45] H. Appelshäuser *et al.* (NA49), Event-by-event fluctuations of average transverse momentum in central Pb + Pb collisions at 158-GeV per nucleon, *Phys. Lett. B* **459**, 679 (1999), [arXiv:hep-ex/9904014](#).
 - [46] D. Adamova *et al.* (CERES), Event by event fluctuations of the mean transverse momentum in 40, 80 and 158 A GeV / c Pb - Au collisions, *Nucl. Phys. A* **727**, 97 (2003), [arXiv:nucl-ex/0305002](#).
 - [47] S. S. Adler *et al.* (PHENIX), Measurement of nonrandom event by event fluctuations of average transverse momentum in s(NN)**(1/2) = 200-GeV Au+Au and p+p collisions, *Phys. Rev. Lett.* **93**, 092301 (2004), [arXiv:nucl-ex/0310005](#).
 - [48] J. Adams *et al.* (STAR), Incident energy dependence of pt correlations at RHIC, *Phys. Rev. C* **72**, 044902 (2005), [arXiv:nucl-ex/0504031](#).
 - [49] T. Anticic *et al.* (NA49), Energy dependence of transverse momentum fluctuations in Pb+Pb collisions at the CERN Super Proton Synchrotron (SPS) at 20A to 158A GeV, *Phys. Rev. C* **79**, 044904 (2009), [arXiv:0810.5580 \[nucl-ex\]](#).
 - [50] S. Acharya *et al.* (ALICE), Skewness and kurtosis of mean transverse momentum fluctuations at the LHC energies, *Phys. Lett. B* **850**, 138541 (2024), [arXiv:2308.16217 \[nucl-ex\]](#).
 - [51] R. Wen, C. Huang, and W.-J. Fu, Baryon number fluctuations in the 2+1 flavor low energy effective model, *Phys. Rev. D* **99**, 094019 (2019), [arXiv:1809.04233 \[hep-ph\]](#).
 - [52] J. Braun, W.-j. Fu, J. M. Pawłowski, F. Rennecke,

- D. Rosenblüh, and S. Yin, Chiral susceptibility in (2+1)-flavor QCD, *Phys. Rev. D* **102**, 056010 (2020), [arXiv:2003.13112 \[hep-ph\]](#).
- [53] J. Braun *et al.*, Soft modes in hot QCD matter, (2023), [arXiv:2310.19853 \[hep-ph\]](#).
- [54] Y.-y. Tan, Y.-r. Chen, W.-j. Fu, and W.-J. Li, Universality of pseudo-Goldstone damping near critical points, *Nature Commun.* **16**, 2916 (2025), [arXiv:2403.03503 \[hep-th\]](#).
- [55] W.-j. Fu, J. M. Pawłowski, R. D. Pisarski, F. Rennecke, R. Wen, and S. Yin, The QCD moat regime and its real-time properties, (2024), [arXiv:2412.15949 \[hep-ph\]](#).
- [56] N. Dupuis, L. Canet, A. Eichhorn, W. Metzner, J. M. Pawłowski, M. Tissier, and N. Wschebor, The nonperturbative functional renormalization group and its applications, *Phys. Rept.* **910**, 1 (2021), [arXiv:2006.04853 \[cond-mat.stat-mech\]](#).
- [57] W.-j. Fu, QCD at finite temperature and density within the fRG approach: an overview, *Commun. Theor. Phys.* **74**, 097304 (2022), [arXiv:2205.00468 \[hep-ph\]](#).
- [58] P. Braun-Munzinger, B. Friman, K. Redlich, A. Rustamov, and J. Stachel, Relativistic nuclear collisions: Establishing a non-critical baseline for fluctuation measurements, *Nucl. Phys. A* **1008**, 122141 (2021), [arXiv:2007.02463 \[nucl-th\]](#).
- [59] V. Vovchenko, V. Koch, and C. Shen, Proton number cumulants and correlation functions in Au-Au collisions at $\sqrt{s_{NN}}=7.7\text{--}200$ GeV from hydrodynamics, *Phys. Rev. C* **105**, 014904 (2022), [arXiv:2107.00163 \[hep-ph\]](#).
- [60] R. Manikandhan (STAR Collaboration), Dynamical transverse momentum fluctuations at high baryon density measured by the STAR Experiment, *Quark Matter 2025*.
- [61] Y. Gao (STAR Collaboration), Collision energy dependence of mean transverse momentum fluctuations in Au+Au collisions at STAR, *Quark Matter 2025*.
- [62] fQCD collaboration, <https://fqcd-collaboration.github.io>.